Author/s:
Pan, B;Huang, Y;Xia, L;Liang, J;Liu, R;Luo, Y;Du, Z;Chen, D;Lam, SK

Title:
Estimating fractions of N2O emissions from nitrification and denitrification using data assimilation

Date:
2025-10-01

Citation:
Pan, B., Huang, Y., Xia, L., Liang, J., Liu, R., Luo, Y., Du, Z., Chen, D. & Lam, S. K. (2025). Estimating fractions of N2O emissions from nitrification and denitrification using data assimilation. Biogeochemistry, 168 (5), pp.71-. https://doi.org/10.1007/s10533-025-01268-x.

Persistent Link:
https://hdl.handle.net/11343/362138

Biogeochemistry (2025) 168:71
https://doi.org/10.1007/s10533-025-01268-x

Estimating fractions of N_2O emissions from nitrification and denitrification using data assimilation

Baobao Pan · Yuanyuan Huang · Longlong Xia · Junyi Liang · Rui Liu · Yiqi Luo · Zhenggang Du · Deli Chen · Shu Kee Lam

Received: 22 March 2025 / Accepted: 27 August 2025 / Published online: 5 September 2025

Abstract Nitrous oxide (N_2O) emissions play a significant role in global warming and stratospheric ozone depletion. Nitrification and denitrification represent the primary pathways of N_2O emissions in agroecosystems. However, modelling the responses of nitrification, denitrification, and subsequent N_2O emissions to soil conditions and nitrification inhibitors remains challenging, as the fractions of N_2O emissions derived from nitrification and denitrification used in model simulations cannot be directly measured. In this study, we estimated soil nitrification, denitrification, N_2O emissions, and their related parameters via data assimilation under various soil moisture levels [water-filled pore space (WFPS) at 50% and 70%], incubation temperature (15, 25 and 35 °C) and nitrification inhibitor application (DMPP, 3MPTZ and C_2H_2) in cereal and vegetable production systems in Australia. We found that the contribution of nitrification to N_2O emissions (i.e., the fraction of N_2O emitted from nitrification, $f_{N_2O\_nit}$) decreased with increasing temperature and moisture content,

Responsible Editor: Edith Bai.

Supplementary Information The online version contains supplementary material available at https://doi.org/10.1007/s10533-025-01268-x.

B. Pan · D. Chen · S. K. Lam (✉)
School of Agriculture, Food and Ecosystem Sciences, Faculty of Science, The University of Melbourne, Parkville, VIC 3010, Australia
e-mail: shukee.lam@unimelb.edu.au

Y. Huang
Institute of Geographic Sciences and Natural Resources Research, Chinese Academy of Sciences, Beijing 100101, China

L. Xia
State Key Laboratory of Soil and Sustainable Agriculture, Institute of Soil Science, Chinese Academy of Sciences, Nanjing 210008, China

J. Liang
Department of Grassland Resource and Ecology, College of Grassland Science and Technology, China Agricultural University, Beijing 100193, China

R. Liu
Beijing Key Laboratory of Farmyard Soil Pollution Prevention-Control and Remediation, College of Resources and Environmental Sciences, China Agricultural University, Beijing 100193, China

Y. Luo
School of Integrative Plant Science, Cornell University, Ithaca, NY 14853, USA

Z. Du
Northeast Asia Ecosystem Carbon Sink Research Centre (NACC), Centre for Ecological Research, Key Laboratory of Sustainable Forest Ecosystem Management-Ministry of Education, School of Forestry, Northeast Forestry University, Harbin 150040, China

whereas denitrification dominated N_2O production (i.e., the fraction of N_2O emitted from denitrification, f_{N2O_dni}) under 70% WFPS regardless of temperatures. Under fertilizer N application, the use of nitrification inhibitors decreased $f_{N_2O\_nit}$ but increased f_{N2O_dni}. The efficacy of nitrification inhibitors in mitigating N_2O emissions varied with environmental conditions. In this study, we demonstrate the use of data assimilation to constrain key parameters for predicting nitrification, denitrification and associated N_2O emissions in response to soil environments and management practices. Integrating this technique into ecosystem process-based models has the potential to enhance model accuracy by reducing uncertainties and biases.

Keywords Data assimilation · N_2O production · Nitrification · Denitrification · Model parameter

Introduction

Nitrous oxide (N_2O) is a potent greenhouse gas contributing to global warming and stratospheric ozone depletion (Butterbach-Bahl et al. 2013). N_2O is primarily produced through nitrification and denitrification (Butterbach-Bahl et al. 2013), which are regulated by soil and environmental factors (Bengtsson et al. 2003; Zebarth et al. 2015; Senbayram et al. 2019). According to a recent global meta-analysis, soil nitrification rate is positively correlated with mean annual temperature, microbial biomass carbon (MBC), soil pH, total nitrogen, and NH_4^+ content, but negatively correlated with the C/N ratio of both soil and microbial biomass (Li et al. 2020). Soil denitrification rate generally increases with soil NO_3^- content, soil temperature and water filled pore space (WFPS) while decreasing with soil oxygen availability (Pan et al. 2022).

Numerous studies have been conducted to investigate nitrification and denitrification processes, their controlling factors and their contributions to N_2O production (Stevens et al. 1997; Wrage et al. 2005; Yu et al. 2020). These studies have significantly advanced our understanding of N cycling including N_2O emission and its mechanisms and have facilitated the model development and validation for simulating N dynamics. The foundational "hole-in-the-pipe" model (Firestone and Davidson 1989) highlights that nitrification rate, denitrification rate, and the proportion of N lost as N_2O are influenced by soil and environmental factors such as water-filled pore space (WFPS) and substrate availability. This model also emphasizes that N_2O is not emitted as a fixed fraction of nitrification or denitrification. However, it is still challenging to estimate the parameters of process-based models based solely on limited experimental data. For example, although modules of N_2O emissions from different pathways have been included in most process-based models, some parameters such as the ratio of N_2O derived from nitrification and denitrification have not been well estimated. A fixed ratio is used in these models to estimate the proportion of N_2O emissions from nitrification and denitrification (Chen et al. 2008), e.g., 0.002 for estimating N_2O emission from nitrification by The Agricultural Production System sIMulator (APSIM; Keating et al. 2003), and 0.5 for N_2O emission from denitrification at 80% WFPS for the Water and Nitrogen Management Model (WNMM; Li et al. 2007). Moreover, the relationships between nitrification, denitrification, their associated N_2O emissions and potential key drivers remain unclear and have been handled inconsistently in existing process-based models (Burke et al. 2003). These unknowns may also result in uncertain predictions of feedback to different N management practices and environmental conditions (Friedlingstein et al. 2014).

Nitrification inhibitors (NIs) e.g., 3-methylpyrazole 1, 2, 4-triazole (3MPTZ; Wolf et al. 2014; Wu et al. 2017), 3, 4-dimethylpyrazole phosphate (DMPP; Zerulla et al. 2001), acetylene (C_2H_2; Hynes and Knowles 1978) etc. are widely used to reduce N_2O emissions (Akiyama et al. 2010; Xia et al. 2017). NIs could delay the oxidation of NH_4^+ to hydroxylamine, the first step of nitrification, thus decreasing the amount of NO_3^-, which is susceptible to leaching and loss through denitrification (Xia et al. 2017). While many process-based models simulate N_2O emissions, their capacity to represent NIs' impact on N cycling is constrained by the lack of an NI module and relevant parameters. Giltrap et al. (2010) adopted an empirical model to simulate nitrification inhibition within the New Zealand Denitrification–Decomposition (NZ-DNDC) model. In this approach, a simplified exponential function was employed to estimate temporal effects of Dicyandiamide (DCD)'s biological degradation. Nevertheless, this empirical model

did not consider soil properties or the application rate of NIs. It is well-established that the efficacy of NIs varies with factors e.g., soil water content and temperature (Menéndez et al. 2012). Further investigation is necessary to identify or refine the module parameters, thereby improving the reliability of model simulation (Cichota et al. 2010; Giltrap et al. 2010; Grant et al. 2020).

Data assimilation enhances the model accuracy and reliability by optimizing model representation align with observational data (Lorenc 1995). It is a statistically rigorous method for estimating uncertainties in model parameters, initial conditions, and state variables, as well as evaluating alternative response functions and model structures (Luo et al. 2011; Luo and Schuur 2020). Through the integration of mathematical process models and empirical experimental data, data assimilation is expected to enhance ecological forecasting (Baker et al. 2010) by estimating parameters and their uncertainties that are not directly measurable through experiments (Li et al. 2013; Schädel et al. 2013). Data assimilation has been widely employed to estimate or refine various parameters or processes associated with C cycling simulations and modellings, e.g., C pool sizes, the response of soil heterotrophic respiration to temperature sensitivity, allocation and transfer coefficients, residence times, and the partitioning of soil autotrophic and heterotrophic respiration. (Zhou and Luo 2008; Zhou et al. 2008, 2010, 2018; Weng et al. 2011; Schädel et al. 2013; Luo et al. 2016; Xu et al. 2016; Guan et al. 2022; Tao et al. 2023). However, the application of data assimilation has not been extended to the N_2O emission simulation. This technique can enhance performance of N_2O modelling by optimizing difficult-to-measure parameters and reducing model uncertainty. Nonetheless, its performance depends on the availability and quality of input data and may be computationally intensive. Here, we applied data assimilation, developed a N_2O model and conducted inverse analysis of data from soil incubation datasets to estimate soil nitrification and denitrification rates, and their relative contributions to N_2O emissions. We aimed to examine the roles of soil moisture content, temperature and NIs in regulating nitrification and denitrification processes in Australian soils. Based on these objectives, we tested the following hypotheses: (1) data assimilation can be used to optimize N_2O associated parameters in N_2O prediction model, (2) parameters constrained by data assimilation can capture the responses of N_2O emissions to NI applications, different soil properties and environmental conditions.

Materials and methods

Dataset of data assimilation

In the study, the datasets were obtained from two incubation experiments, Liu et al. (2015, 2017). Details on the sites and soil properties were provided in Table 1. Experiment 1 investigated the effect of NIs (3MPTZ, DMPP) on mineral N dynamics, N_2O and CO_2 fluxes in a vegetable farm (Boneo, Victoria, Australia). This incubation experiment included four treatments (control; fertilizer N; N + 3MPTZ; N + DMPP), conducted at 25 °C and 60% WFPS. Experiment 2 investigated the effects of NI (1% v/v acetylene, C_2H_2), incubation temperature (15 °C, 25 °C and 35 °C and soil moisture (50% and 70% WFPS) on mineral N dynamics, N_2O and CO_2 fluxes in a cropland (Hamilton, Victoria, Australia). Soil samples were air-dried, ground and sieved (< 2 mm) before analysis and incubation experiments. Each treatment was applied with 150 mg N kg^{-1} (^{15}N at 10% atom excess) except for the control treatment. For both experiments, soil NO_3–N and NH_4–N measured on days 0, 6, 14, 23, 28, and 42. Total N_2O and CO_2 fluxes were measured on days 0, 2, 4, 6, 11, 21,

Table 1 Basic site description and soil physicochemical properties used in incubation studies

Land use	Site name	Location	Texture	Clay (%)	pH	NH_4–N (mg N kg^{-1})	NO_3–N (mg N kg^{-1})	Organic carbon (%)	Total nitrogen (%)
Vegetable	Boneo	38.3°S, 144.9°E	Sand	1	7.9	1.1	19	0.64	0.08
Cropping	Hamilton	38.3°S, 142.1°E	Loam	10	7.0	5.1	10	6.2	0.52

and 26. These observation data were used for model development and validation ("Model description" and "Data assimilation" sections).

Model description

Daily soil nitrification and denitrification rates, as well as their contributions to N_2O emissions under different soil temperature, moisture and nitrification inhibitors were modelled in a carbon–nitrogen coupled N_2O model (Fig. S1, Eqs. 1–15). The model contains two main components, viz. the C cycle and the N component. Soil organic C exists in various forms and its dynamics is typically represented by multiple C pools (Trumbore 1997). This model was developed to distinguish the measured CO_2 emissions in experiments by separating it into two C pools: the particulate and mineral-associated organic C pools (POC and MOC, respectively) based on the different decomposability (POC > MOC), and C transferred between these pools. Since POC and MOC were not directly measured in the incubation experiments, their initial proportions were treated as model parameters and inferred from total organic C. The transfer of C among pools also regulates the amount of N available, because the mineralization process determines NH_4^+ release and thereby links the C–N cycle by affecting C:N ratios of these pools (Schädel et al. 2013). In each treatment, the C decomposition flux is modelled as D_{co_2}, the sum of all decomposition fluxes d_{co_2} from C-pools C_i (Eqs. 1, 2) as:

$$D_{co_2} = \sum_{i=1}^{I} d_{co_2,\ i} = \sum_{i=1}^{I} q_i \cdot C_{tot} \cdot f_i \tag{1}$$

$$q_i = \alpha_i \cdot e^{-\alpha_i \cdot t}, i\epsilon\{1, \ldots, I\}, \tag{2}$$

where D_{co_2} denotes the total CO_2 emission resulting from decomposition; i represents the number of C pools ($i = 1$ or 2); C_{tot} represents the initial total C pool prior to decomposition; f_i^C (Eq. 4 $0 \le f_i^C \le 1$ and $\sum_{i=1}^{I} f_i^C = 1$) is the initial proportion of the ith pool within C_{tot}; the parameter α_i denotes the constant of decomposition rate of the ith pool; while t represents the decomposition duration in days. As constants of decomposition rate α_i are temperature dependent, functions of temperature response (Eq. 3) were adopted to represent rates of decomposition under different temperatures (T, $T = 15$, 25, 35 °C).

$$\alpha_i = k_i Q_{10}{}^{(T-25)/10}, \tag{3}$$

$$f_i^C = \frac{C_i}{C_{tot}}, i\epsilon\{1, \ldots, I\}. \tag{4}$$

In the N component, the total N mineralization flux (N_{min}) that is the sum of n_{min} can be modelled in Eqs. 5–8 as:

$$N_{min} = \sum_{i=1}^{I} n_{min,i} = \sum_{i=1}^{I} s_i \cdot N_{tot} \cdot f_i^N, \tag{5}$$

$$s_i = \alpha_i \cdot N_{C_i} \cdot e^{-\alpha_i \cdot t \cdot N_{C_i}}, i\epsilon\{1, \ldots, I\}, \tag{6}$$

$$f_i^N = \frac{N_i}{N_{tot}}, i\epsilon\{1, \ldots, I\}, \tag{7}$$

$$\sum_{i=1}^{I} f_i^C = \sum_{i=1}^{I} f_i^N = 1, \tag{8}$$

where N_{tot} is the total available N for mineralization. f_I' (Eq. 5, $0 \le f_i' \le 1$ and $\sum_{i=1}^{I} f'_i = 1$) represents the initial proportion of the ith pool in N_{tot}; N_C_i is the C/N ratio.

In this model, we adopted the generally accepted conceptual "hole-in-the-pipe" framework to distinguish between the two main N_2O emission pathways: nitrification and denitrification (Firestone and Davidson 1989). This conceptual idea can be found in many process-based models and described as first-order kinetics (WNMM, Li et al. 2007) or Michaelis–Menten kinetics (APSIM, Keating et al. 2003) and different input variables and functions were used in these two processes. Nitrification (N_{nit}) and denitrification (N_{dni}) rates can be calculated by Eqs. 9–15 as:

$$N_{nit} = \beta_n \cdot NH_4^+ \tag{9}$$

$$N_{dni} = \beta_d \cdot NO_3^- \tag{10}$$

$$\beta_n = k_n \cdot Q_n^{(T-25)/10} \tag{11}$$

Table 2 Maximum likelihood estimates (MLEs) or means (for unconstrained parameters) of parameter values

Treatment/ parameter	Control	N fertilizer	N+DMPP	N+3MPTZ	N treatment (50% WFPS)	N+C_2H_2 (50% WFPS)	N treatment (70% WFPS)	N+C_2H_2 (70% WFPS)
f_1 (%)	$1.94\times10^{-2}\pm1.06\times10^{-2}$	$8.61\times10^{-2}\pm1.04\times10^{-2}$	$1.4\times10^{-2}\pm1.23\times10^{-2}$	$1.38\times10^{-2}\pm1.14\times10^{-2}$	$2.34\times10^{-2}\pm2.45\times10^{-2}$	$2.18\times10^{-2}\pm1.72\times10^{-2}$	$2.64\times10^{-2}\pm2.64\times10^{-2}$	$1.45\times10^{-2}\pm1.16\times10^{-2}$
K_1 (mg C g^{-1} day^{-1})	$2.15\times10^{-2}\pm1.67\times10^{-2}$	$1.38\times10^{-2}\pm3.5\times10^{-3}$	$2.03\times10^{-2}\pm1.81\times10^{-2}$	$1.79\times10^{-2}\pm1.77\times10^{-2}$	$1.31\times10^{-2}\pm9.8\times10^{-3}$	$2.68\times10^{-2}\pm2.13\times10^{-2}$	$1.43\times10^{-2}\pm1.39\times10^{-2}$	$1.98\times10^{-2}\pm1.5\times10^{-2}$
K_2 (mg C g^{-1} day^{-1})	$2\times10^{-4}\pm1\times10^{-4}$	$3\times10^{-4}\pm2\times10^{-4}$	$3\times10^{-4}\pm1\times10^{-4}$	$3\times10^{-4}\pm1\times10^{-4}$	$9\times10^{-4}\pm1\times10^{-4}$	$8\times10^{-4}\pm1\times10^{-4}$	$1.2\times10^{-3}\pm2\times10^{-4}$	$1.1\times10^{-3}\pm1\times10^{-4}$
Q1@15	–	–	–	–	1.75 ± 0.55	2.37 ± 0.67	2.82 ± 1.42	2.3 ± 0.95
Q2@15	–	–	–	–	3.85 ± 0.47	4.26 ± 0.72	3.29 ± 0.23	2.84 ± 0.35
Q1@25	–	–	–	–	2.57 ± 0.61	1.72 ± 0.53	1.62 ± 0.41	1.64 ± 0.55
Q2@25	–	–	–	–	1.54 ± 0.24	2.22 ± 0.36	1.2 ± 0.16	1.32 ± 0.18
N_C_1 (mg N kg^{-1} day^{-1})	0.61 ± 0.12	$0.86\pm6.59\times10^{-2}$	0.45 ± 0.27	0.3 ± 0.11	0.29 ± 0.13	$0.28\pm8.83\times10^{-2}$	0.17 ± 0.13	0.27 ± 0.12
k_n (mg N kg^{-1} day^{-1})	$5.17\times10^{-2}\pm1.3\times10^{-2}$	$0.41\pm5.09\times10^{-2}$	$4.7\times10^{-2}\pm1.36\times10^{-2}$	$3.58\times10^{-2}\pm1.08\times10^{-2}$	$4.6\times10^{-3}\pm1.7\times10^{-3}$	$3.3\times10^{-3}\pm8\times10^{-4}$	$3.26\times10^{-2}\pm8.9\times10^{-3}$	$1.11\times10^{-2}\pm3.9\times10^{-3}$
Q_n					1.23 ± 0.19	$0.63\pm9.74\times10^{-2}$	4.94 ± 0.45	3.29 ± 0.66
k_d	$1.83\times10^{-2}\pm1.2\times10^{-2}$	$4.99\times10^{-2}\pm7.6\times10^{-3}$	$6\times10^{-3}\pm3.7\times10^{-3}$	$5.8\times10^{-3}\pm4\times10^{-3}$	$1.3\times10^{-3}\pm7\times10^{-4}$	$1.2\times10^{-3}\pm1\times10^{-3}$	$2.88\times10^{-2}\pm8\times10^{-3}$	$9.8\times10^{-3}\pm5.4\times10^{-3}$
Q_d					4.12 ± 0.58	3.03 ± 0.99	9.2 ± 0.52	9.43 ± 0.44
f_{N2O_nit}	0.3 ± 0.16	0.23 ± 0.1	$2.01\times10^{-2}\pm1.62\times10^{-2}$	$6.59\times10^{-2}\pm4.68\times10^{-2}$	$2.3\times10^{-3}\pm1.5\times10^{-3}$	$2\times10^{-3}\pm7\times10^{-4}$	$4.9\times10^{-3}\pm3.8\times10^{-3}$	$2\times10^{-3}\pm1.4\times10^{-3}$
f_{N2O_dni}	$2.42\times10^{-2}\pm1.47\times10^{-2}$	0.18 ± 0.12	0.35 ± 0.19	0.39 ± 0.23	$8.1\times10^{-3}\pm6.6\times10^{-3}$	$7.8\times10^{-3}\pm7.6\times10^{-3}$	$5.33\times10^{-2}\pm2.06\times10^{-2}$	$8.48\times10^{-2}\pm6.4\times10^{-2}$

Values are reported as MLEs or mean ± standard deviation (SD)

$$\beta_d = k_d \cdot Q_d^{(T-25)/10} \tag{12}$$

$$\frac{d\mathrm{NH}_4^+}{dt} = N_{input} + N_{min} - N_{nit}, \tag{13}$$

$$\frac{d\mathrm{NO}_3^-}{dt} = N_{input} + N_{nit} - N_{dni}, \tag{14}$$

$$N_2O = f_{\mathrm{N_2O\_nit}} \cdot N_{nit} + f_{N2O\_dni} \cdot N_{dni}. \tag{15}$$

k_n and k_d represent the base rate constants (at 25 °C) for nitrification and denitrification while Q_n and Q_d are their respective Q_{10} coefficients. N_{input} denotes the N application rate applied to the soil. N_2O can be simply modelled as a sum of N_2O release from both nitrification (NH_4^+ pool) and denitrification (NO_3^- pool) (Eq. 15), where $f_{\mathrm{N_2O\_nit}}$ and f_{N2O_dni} are the fractions of N_2O emission from nitrification and denitrification, respectively.

Data assimilation

To better simulate C and N dynamics in this N_2O model ("Model description" section), we used data assimilation to optimize the parameters associated with the model and thus to improve model prediction. In this study, Bayesian probabilistic inversion (Eq. 16) was employed to constrain parameters in C and N dynamics (Xu et al. 2006).

$$P(p|Z) \propto P(Z|p)P(p). \tag{16}$$

The posterior probability distribution of parameters (p), denoted as $P(p|Z)$, is derived from prior information, which is described by the prior probability distribution $P(p)$ and dataset-derived information, represented through the likelihood function $P(Z|p)$. The prior probability of estimated parameters was modelled following a uniform distribution across predefined intervals. Parameters related to N_2O emissions (i.e., nitrification rate, denitrification rate, fraction of N_2O emitted from nitrification and denitrification, Q_{10} at different temperatures) and key parameters of initial C pools, C decomposition rates were simultaneously constrained by the approach of Bayesian probabilistic inversion (Table 2). The ranges of *prior* parameter values were determined by prior knowledge.

The likelihood function $P(Z|p)$ was computed assuming that errors between observed and modelled data follow an independently and normally distributed Gaussian distribution, expressed as follows (Eq. 17)

$$P(Z|p) \propto \exp\left\{ -\frac{1}{2\sigma^2} \sum_{t \epsilon obs(Z_i)} \left[Z_i(t) - X_i(t)\right]^2 \right\}, \tag{17}$$

where σ is the standard deviation of the observed measurements, $Z(t)$ represents the observed measurements data at time t, and $X(t)$ denotes the corresponding simulated value. The Metropolis–Hastings (M–H) algorithm was applied in probabilistic inversion to estimate the posterior probability density functions (PDFs) of model parameters. In brief, the M–H algorithm enables the sampling of random variables within high-dimensional probability distributions by applying a Markov Chain Monte Carlo (MCMC)-based approach (Metropolis et al., 1953; Hastings, 1970; Li et al. 2013). It operates through an iterative process involving two main steps: a proposal step, where a new candidate point p^{new} is generated for the parameter vector p using the previously accepted p^{old}, and a movement step, where the candidate is evaluated for acceptance based on a proposal distribution $P(p^{new}|p^{old})$ (Eq. 18):

$$p^{new} = p^{old} + d(p_{max} - p_{min})/D \tag{18}$$

where p_{max} and p_{min} are the maximum and minimum values, respectively, within the prior distribution of the parameter. In each movement step, p^{new} was evaluated using the Metropolis criterion to determine its acceptance or rejection (Xu et al. 2006). The M–H algorithm iteratively repeated the proposal and movement steps until a sufficient number of parameter sets had been accepted. To illustrate parameter distributions within the parameter space, PDFs were generated for each parameter. The maximum likelihood estimates (MLEs) of each parameter or mean values (if the parameter is not well constrained) were used to simulate CO_2 and N_2O emissions.

The model was then validated based on the posterior optimal parameters derived from data assimilation. A hold-out validation was implemented, where 80% of the observational data were used for model fitting, and the remaining 20% were reserved for validation (Arlot 2010). Model predictions based on the

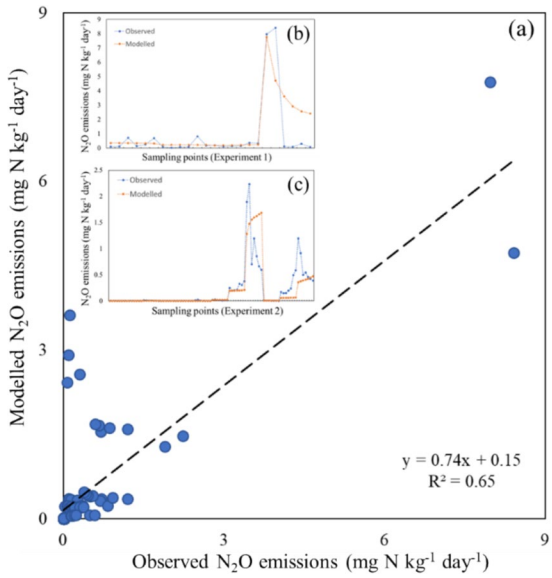

Fig. 1 **a** Scatter plot of the measured against simulated N_2O emission by data assimilation. Insets **b** and **c** show the observed and modelled N_2O emissions at each sampling point in Experiments 1 and 2, respectively

fitted parameters were evaluated against the held-out data using overall R^2 metrics. To evaluate model uncertainty, we used the optimized parameter sets to simulate an ensemble of model outputs. For each time point and variable, we calculated the median prediction and the 95% confidence interval (2.5th to 97.5th percentiles) across all accepted simulations. Sensitivity analysis was conducted to quantify the influence of each parameter on the predicted N_2O flux. Each parameter was perturbed by ± 20% around its simulated value while others were held constant (Shi et al. 2016). The sensitivity index was defined as the relative change in N_2O flux compared to the baseline simulation (Figs. S3–S10). A least significant difference (LSD) test was performed to compare the differences in nitrification, denitrification and N_2O emission between treatments. SPSS was used to conduct all analyses (Version 25, SPSS, Inc., Chicago, IL, USA).

Results

Model parameters are categorized into well-constrained, poorly constrained, and edge-hitting according to their shapes of posterior PDFs (Luo et al. 2009). Here, most parameters across three datasets were well constrained (Figs. S3–S10). However, f_{N2O_dni} in the control treatment (Fig. S3) and N_C_1 was not constrained in two NI treatments in experiment 2 (Figs. S9, S10). For well-constrained parameters, an MLE was estimated, whereas a mean value was used for poorly constrained ones (Table 2). $f_{N_2O\_nit}$ and f_{N2O_dni} varied with N treatments. $f_{N_2O\_nit}$ was higher in the control (0.3) and N fertilizer (0.23) treatment than N + 3MPTZ (0.066) and N + DMPP (0.02). On the contrary, f_{N2O_dni} was higher in

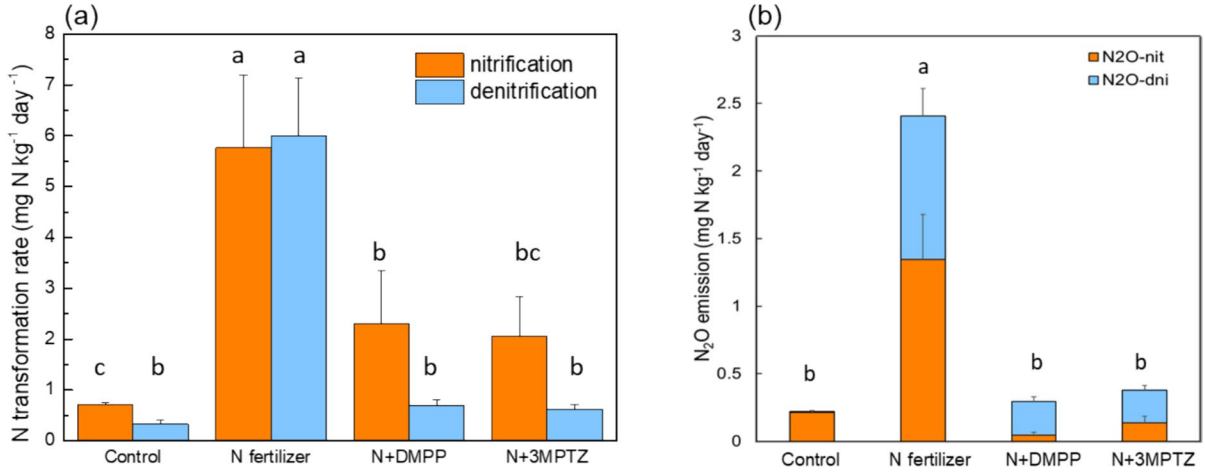

Fig. 2 Modelled nitrification rate, denitrification rate (**a**) and associated N_2O emissions (**b**) in Experiment 1. Different letters in the figure indicated the statistically significant differences at the $p < 0.05$ level

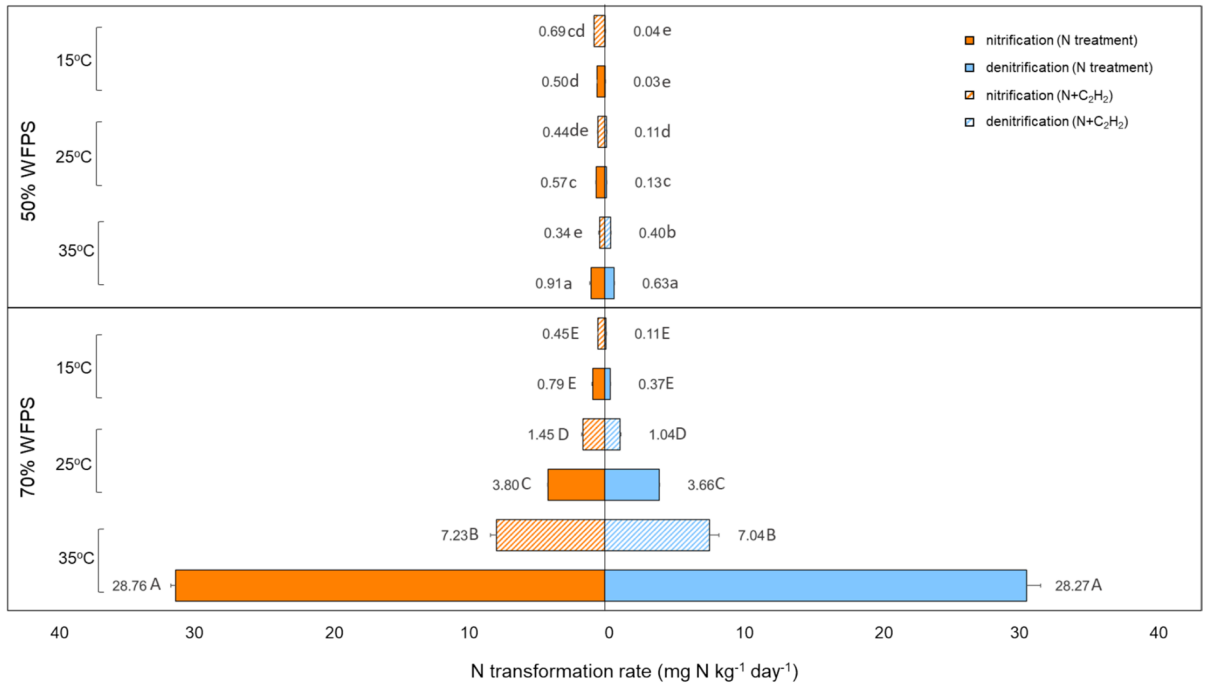

Fig. 3 Modelled nitrification and denitrification rates at different moisture contents (50 and 70% WFPS) and temperatures (15 °C, 25 °C and 35 °C) in Experiment 2. Different letters in the figure indicated the statistically significant differences at the $p < 0.05$ level, capital and lower-case letters indicate two moisture contents

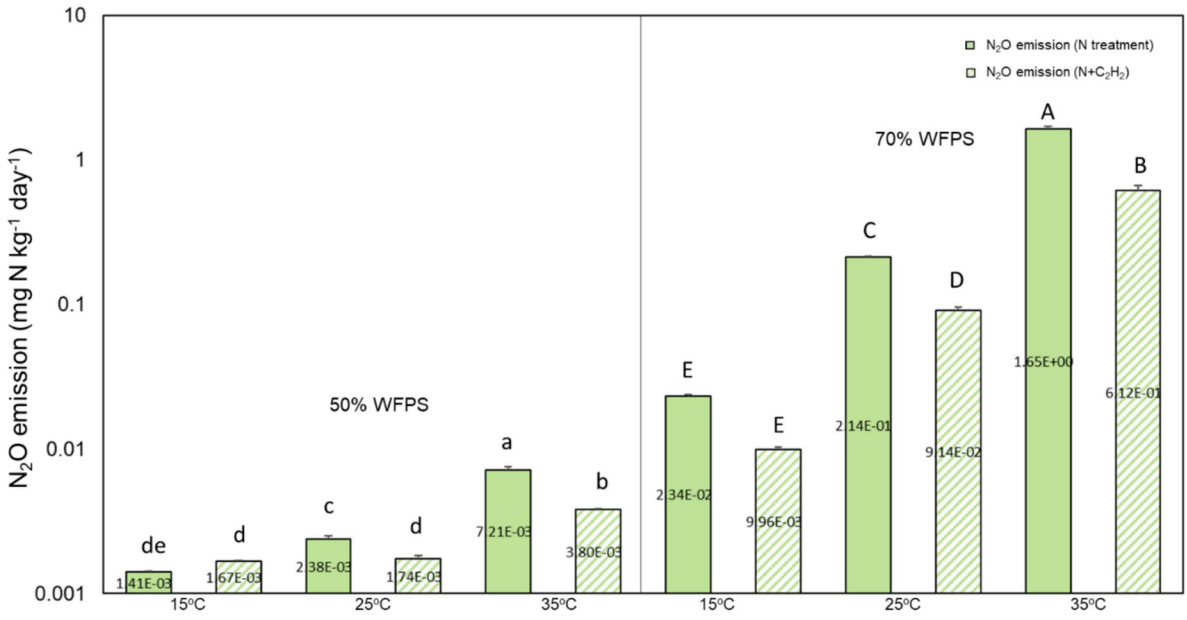

Fig. 4 Modelled N_2O emission from nitrification and denitrification at different moisture contents (50 and 70% WFPS) and temperatures (15 °C, 25 °C and 35 °C) in Experiment 2. Different letters in the figure indicated the statistically significant differences at the $p < 0.05$ level, capital and lower-case letters indicate two moisture contents

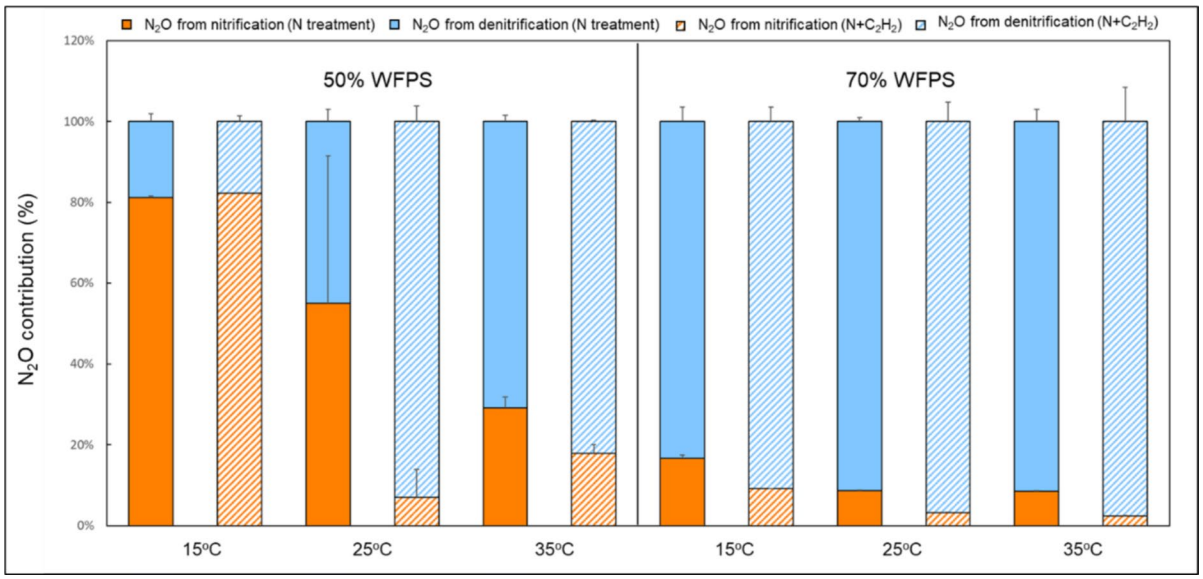

Fig. 5 Nitrification and denitrification contributions to N_2O emission at different moisture contents (50 and 70% WFPS) and temperatures (15 °C, 25 °C and 35 °C) in Experiment 2

N + 3MPTZ (0.39) and N + DMPP (0.35) than the control (0.02) and N fertilizer treatment (0.18). Overall, the model achieved a reliable prediction performance of N_2O emission with an R^2 of 0.65 (Fig. 1).

In Fig. 2a, the nitrification and denitrification rates were the lowest for the control (0.7 mg N kg^{-1} day^{-1} and 0.3 mg N kg^{-1} day^{-1}, respectively) but highest under the N fertilizer treatment (5.8 mg N kg^{-1} day^{-1} and 6.0 mg N kg^{-1} day^{-1}, respectively). When N fertilizer was applied with NIs, nitrification and denitrification rates were significantly decreased by 60–64% and 88–90%, respectively. Fertilizer treatment had the highest N_2O emission per day with an average of 2.4 mg N kg^{-1}, followed by N + 3MPTZ, N + DMPP and the control (0.4 mg N kg^{-1} day^{-1}, 0.3 mg N kg^{-1} day^{-1} and 0.2 mg N kg^{-1} day^{-1}, respectively, Fig. 2b). Nitrification dominated the N_2O production (96% and 56% for control and N fertilizer, respectively). With the application of NIs, the contribution of denitrification to N_2O emissions increased and became predominant in N + DMPP and N + 3MPTZ (84% and 64%, respectively).

The highest nitrification and denitrification rates occurred at 35 °C and 70% WFPS (28.8 and 28.3 mg N kg^{-1} day^{-1}, respectively, Fig. 3). The application of NIs generally decreased both nitrification and denitrification rates.

Total N_2O emission increased with higher temperature and moisture content (Fig. 4). NI effectively decrease N_2O emissions by 27–63%. The contribution of nitrification to N_2O emissions decreased with increasing moisture content and temperature. Denitrification dominated N_2O production at 70% WFPS regardless of temperatures (Fig. 5).

Discussion

This study explores the integration of data assimilation into process-based modelling to quantify soil nitrification, denitrification processes and associated N_2O emissions. By incorporating observed experimental data to optimize key model parameters, we reduced uncertainties commonly associated with traditional modeling approaches. The following sections detail the model's performance with data assimilation in estimating nitrification and denitrification rates, assessing the effectiveness of NIs, and identifying the environmental factors that regulate N_2O emission pathways.

Performance of model and data assimilation analysis

The successful application of data assimilation in refining key parameters, such as nitrification and denitrification rates and the impact of NIs on N_2O emissions, demonstrates its potential to improve the accuracy of process-based models beyond traditional fixed-ratio approaches. Traditional incubation studies (Liu et al. 2015, 2017) cannot quantify key parameters such as k_n, k_d, Q_n, and Q_d in nitrification and denitrification processes. However, data assimilation combined with empirical modeling and experimental observations enables the estimation of these parameters and associated uncertainties, providing a more comprehensive understanding of these N transformation processes. To our knowledge, this is the first study using data assimilation and mathematical model approach to estimate N_2O production pathways and $f_{N_2O\_nit}$ and f_{N2O_dni}. The satisfactory modelling performance indicated that data assimilation can be used to predict N_2O emissions (overall $R^2 = 0.65$, Fig. 1; Fig. S2) and associated parameters (Table 2). Moreover, for each treatment simulated in this study, the high goodness-of-fit ($R^2 = 0.93$ to 0.97, Figs. S3–S10) and well-constrained model parameters further showed that data assimilation effectively captured the varying responses of nitrification rate, denitrification rate and associated N_2O emissions to soil conditions, environmental factors and NI application.

By adjusting the values of these parameters and updating their probability distribution, parameters used in process-based models can be predicted with reduced uncertainties. For example, $f_{N_2O\_nit}$, a crucial variable for estimating N_2O emission from nitrification, was set to a fixed value in many process-based models (Keating et al. 2003; Li et al. 2007), regardless of geographical location. However, we found that this ratio varied widely (0.002–0.3) with soil moisture and temperature, as well as fertilizer and NI application (Table 2), further corroborating the argument that $f_{N_2O\_nit}$ should be site-specifically adjusted in process-based models (Chen et al. 2008; Pan et al. 2021). The results demonstrate that most parameters were well constrained by datasets derived from incubation studies, but some parameters e.g., f_{N2O_dni} was not well constrained in the control (Fig. S7). This could be attributed to the very small amount of N_2O producing from denitrification from the control, making it challenging for the model to constrain parameters with weak signals (Xu et al. 2016).

Contributions of nitrification and denitrification to N_2O emissions under various soil conditions and nitrification inhibitors

The estimated parameters (k_n, k_d, $f_{N_2O\_nit}$ and f_{N2O_dni}) varied across treatments, reflecting microbial responses of N_2O production to soil/environmental and management conditions. These variations, consistent with known biogeochemical mechanisms, support the model's capacity to capture process-level responses via data assimilation.

Increased N mineralization stimulated by higher temperature can provide more inorganic N as the substrate for nitrification and denitrification (Li et al. 2020). Higher temperature can also stimulate soil respiration rate, providing anaerobic sites to boost denitrification and associated N_2O emissions (Butterbach-Bahl and Dannenmann 2011). Moreover, nitrification's contribution to N_2O emissions declined as temperature increased (Fig. 5), which might be attributed to the tendency of nitrite to accumulate at low temperatures (Maag and Vinther 1996). k_d and Q_d were significantly higher in the 70% WFPS treatments. This suggests denitrification dominated N_2O emissions at 70% WFPS (Fig. 5) due to increased microbial activity (Fig. 4) resulting from oxygen depletion at high soil moisture. (Davidson et al. 2000).

The estimated k_n was highest under the fertilizer-only treatment, reflecting the abundant NH_4^+ supply that stimulated autotrophic ammonia oxidizers. In contrast, our simulation results showed that total N_2O emissions decreased by 27–88% when NIs were used in the vegetable and cropping systems (Figs. 2b, 4). The percent reduction is within the range of emission reduction observed in agricultural systems (Li et al. 2018; Lam et al. 2022). We observed significant reduction of k_n, $f_{N_2O\_nit}$ and associated N_2O emission from nitrification under NI application (Fig. 2; Table 2), likely resulting from the inhibition of ammonia monooxygenase by DMPP, 3MPTZ and C_2H_2 (Ruser and Schulz 2015). Under inhibitor treatments, k_d also decreased. The inhibitory effect of NIs on denitrification and associated N_2O was attributed to their indirect influence on denitrification enzyme activity. (Müller et al. 2002).

Soil denitrification-derived N_2O emissions were decreased by the reduced substrate (NO_3^-) availability for denitrifying organisms (Ruser and Schulz 2015; Wu et al. 2017) (Fig. 2). Notably, the ability of NIs to mitigate N_2O emissions varies with environmental factors, especially soil moisture and temperature, as demonstrated in prior research (Maag and Vinther 1996; Menéndez et al. 2012) and the present study. For example, we found that NI (C_2H_2) was more effective under higher soil water content and temperature (Fig. 4). This agrees with Wu et al. (2017), who found that NIs were more effective in reducing N_2O emissions under the conditions favouring denitrification, such as high labile C content and soil moisture. In this regard, the choice of NIs needs to be tailored for specific soil type and environmental conditions (Lam et al. 2022).

Data assimilation successfully simulated the responses of N transformation rates and N_2O emissions to NI application (Figs. 2b, 5), providing insights into how N management (e.g., NI application) reduces N_2O emissions through affecting nitrification and denitrification processes under diverse soils and climates. As such, data assimilation could be embedded into process-based models (Gurung et al. 2021; Kivi et al. 2022) to build a new module for simulating the inhibitory effect of NIs, and possibly expandable to other management strategies, on N_2O emissions. Indeed, recent studies have demonstrated that combining neural networks with data assimilation enhances soil C storage simulations in land biogeochemical models (Tao et al. 2020, 2023; Xia et al. 2020). Data assimilation refines machine learning models by optimizing parameters and associated uncertainties, addressing ambiguities stemming from observational limitations in soil C–N cycling simulations (Geer 2021).

However, limitations and uncertainties still exist. The limited short-term incubation data may make it challenging to constrain some parameters as it may not fully reflect the N_2O emission response over a longer term. The model performance can be improved when more long-term data is available. Besides, other microbial processes such as nitrifier denitrification, dissimilatory nitrate reduction to ammonium (DNRA), co-denitrification and chemical processes (e.g., chemo-denitrification)may have also contributed to N_2O production and led to uncertainty in the current estimation (Hu et al. 2015). In this model, only nitrification and denitrification were considered, resulting in uncertainties in estimating N_2O production from different pathways. Data assimilation has been successfully applied to in situ and large-scale datasets in C cycle studies (e.g., Weng et al. 2011; Zhou and Luo 2008). Its application in N cycle modelling remains limited. Our study demonstrates its potential, and future work could integrate diverse field measurements to enhance parameter estimation and model performance under real-world conditions.

Conclusion

We first attempted to incorporate data assimilation techniques into a N_2O model for estimating nitrification, denitrification and their associated N_2O production under different soil conditions and the use of NIs. Important parameters such as $f_{N_2O\_nit}$, f_{N2O_dni}, Q_{10} were optimized with data assimilation analysis. The model reliably predicted N_2O emissions from nitrification and denitrification, the contributions of these processes to the emissions, as well as the responsiveness of parameters to diverse soil environmental conditions and the use of nitrification inhibitors. Our findings suggest that data assimilation could potentially be embedded into process-based models to reduce model uncertainties and associated errors with N_2O prediction, and to facilitate development of new module targeting N management practices. This advancement benefits the understanding and simulations of terrestrial C and N dynamics.

Acknowledgements We thank Dr. Xiaoyu Xia and Dr. Bo Li for their technical support with MATLAB.

Author contributions All authors contributed to the study. Model conception and design were performed by Baobao Pan, Yuanyuan Huang, Junyi Liang and Shu Kee Lam. Data analysis were performed by Baobao Pan. Data collection was performed by Rui Liu. The first draft of the manuscript was written by Baobao Pan and all authors commented on previous versions of the manuscript. All authors read and approved the final manuscript.

Funding Open Access funding enabled and organized by CAUL and its Member Institutions. This work is supported by the Australian Research Council Discovery Project (DP230101787) and the Industrial Transformation Research Hub for Innovative Nitrogen Fertilizers and Inhibitors (IH200100023).

Data availability The raw datasets and MATLAB code used during the current study are available from https://github.com/Baobao5Pan/DataAssimilation.

Declarations

Conflict of interest The authors declare no conflict of interest.

References

Akiyama H, Yan X, Yagi K (2010) Evaluation of effectiveness of enhanced-efficiency fertilizers as mitigation options for N_2O and NO emissions from agricultural soils: meta-analysis. Glob Change Biol 16:1837–1846

Arlot S (2010) A survey of cross-validation procedures for model selection. Stat Surv 4:40–79

Baker D, Bösch H, Doney S, O'Brien D, Schimel D (2010) Carbon source/sink information provided by column CO_2 measurements from the Orbiting Carbon Observatory. Atmos Chem Phys 10:4145–4165

Bengtsson G, Bengtson P, Mansson KF (2003) Gross nitrogen mineralization-, immobilization-, and nitrification rates as a function of soil C/N ratio and microbial activity. Soil Biol Biochem 35:143–154

Burke IC, Kaye JP, Bird SP, Hall SA, McCulley RL, Sommerville GL (2003) Evaluating and testing models of terrestrial biogeochemistry: the role of temperature in controlling decomposition. In: Models in ecosystem science. Princeton University Press, Princeton, pp 225–253

Butterbach-Bahl K, Dannenmann M (2011) Denitrification and associated soil N_2O emissions due to agricultural activities in a changing climate. Curr Opin Environ Sustain 3:389–395

Butterbach-Bahl K, Baggs EM, Dannenmann M, Kiese R, Zechmeister-Boltenstern S (2013) Nitrous oxide emissions from soils: how well do we understand the processes and their controls? Philos Trans R Soc Lond B 368:20130122

Chen D, Li Y, Grace P, Mosier AR (2008) N_2O emissions from agricultural lands: a synthesis of simulation approaches. Plant Soil 309:169–189

Cichota R, Vogeler I, Snow V, Shepperd M (2010) Modelling the effect of a nitrification inhibiter on N leaching from grazed pastures. Proc N Z Grassl Assoc 72:43–47

Davidson EA, Verchot LV, Cattanio JH, Ackerman IL, Carvalho JEM (2000) Effects of soil water content on soil respiration in forests and cattle pastures of eastern Amazonia. Biogeochemistry 48:53–69

Firestone MK, Davidson EA (1989) Microbiological basis of NO and N_2O production and consumption in soil. Wiley, New York

Friedlingstein P, Meinshausen M, Arora VK, Jones CD, Anav A, Liddicoat SK, Knutti R (2014) Uncertainties in CMIP5 climate projections due to carbon cycle feedbacks. J Clim 27:511–526

Geer A (2021) Learning earth system models from observations: machine learning or data assimilation? Philos Trans R Soc Lond A 379:20200089

Giltrap DL, Singh J, Saggar S, Zaman M (2010) A preliminary study to model the effects of a nitrification inhibitor on nitrous oxide emissions from urine-amended pasture. Agric Ecosyst Environ 136:310–317

Grant RF, Lin S, Hernandez-Ramirez G (2020) Modelling nitrification inhibitor effects on N_2O emissions after fall- and spring-applied slurry by reducing nitrifier NH_4^+ oxidation rate. Biogeosciences 17:2021–2039

Guan X, Jiang J, Jing X, Feng W, Luo Z, Wang Y, Xu X, Luo Y (2022) Optimizing duration of incubation experiments for understanding soil carbon decomposition. Geoderma 428:116225

Gurung RB, Ogle SM, Breidt FJ, Parton WJ, Del Grosso SJ, Zhang Y, Hartman MD, Williams SA, Venterea RT (2021) Modeling nitrous oxide mitigation potential of enhanced efficiency nitrogen fertilizers from agricultural systems. Sci Total Environ 801:149342

Hu H-W, Chen D, He J-Z (2015) Microbial regulation of terrestrial nitrous oxide formation: understanding the biological pathways for prediction of emission rates. FEMS Microbiol Rev 39:729–749

Hynes RK, Knowles R (1978) Inhibition by acetylene of ammonia oxidation in *Nitrosomonas europaea*. FEMS Microbiol Lett 4:319–321

Keating BA, Carberry PS, Hammer GL, Probert ME, Robertson MJ, Holzworth D, Huth NI, Hargreaves JN, Meinke H, Hochman Z (2003) An overview of APSIM, a model designed for farming systems simulation. Eur J Agron 18:267–288

Kivi MS, Blakely B, Masters M, Bernacchi CJ, Miguez FE, Dokoohaki H (2022) Development of a data-assimilation system to forecast agricultural systems: a case study of constraining soil water and soil nitrogen dynamics in the APSIM model. Sci Total Environ 820:153192

Lam SK, Wille U, Hu H-W, Caruso F, Mumford K, Liang X, Pan B, Malcolm B, Roessner U, Suter H (2022) Next-generation enhanced-efficiency fertilizers for sustained food security. Nat Food 3:575–580

Li Y, White R, Chen D, Zhang J, Li B, Zhang Y, Huang Y, Edis R (2007) A spatially referenced water and nitrogen management model (WNMM) for (irrigated) intensive cropping systems in the North China Plain. Ecol Model 203:395–423

Li D, Schädel C, Haddix ML, Paul EA, Conant R, Li J, Zhou J, Luo Y (2013) Differential responses of soil organic

carbon fractions to warming: results from an analysis with data assimilation. Soil Biol Biochem 67:24–30
Li T, Zhang W, Yin J, Chadwick D, Norse D, Lu Y, Liu X, Chen X, Zhang F, Powlson D (2018) Enhanced-efficiency fertilizers are not a panacea for resolving the nitrogen problem. Glob Change Biol 24:e511–e521
Li Z, Zeng Z, Tian D, Wang J, Fu Z, Zhang F, Zhang R, Chen W, Luo Y, Niu S (2020) Global patterns and controlling factors of soil nitrification rate. Glob Change Biol 26(7):4147–4157
Liu R, Hayden H, Suter H, He J, Chen D (2015) The effect of nitrification inhibitors in reducing nitrification and the ammonia oxidizer population in three contrasting soils. J Soils Sediments 15:1113–1118
Liu R, Hayden HL, Hu H, He J, Suter H, Chen D (2017) Effects of the nitrification inhibitor acetylene on nitrous oxide emissions and ammonia-oxidizing microorganisms of different agricultural soils under laboratory incubation conditions. Appl Soil Ecol 119:80–90
Lorenc AC (1995) Atmospheric data assimilation. Meteorological Office, Berkshire
Luo Y, Schuur EA (2020) Model parameterization to represent processes at unresolved scales and changing properties of evolving systems. Glob Change Biol 26:1109–1117
Luo Y, Weng E, Wu X, Gao C, Zhou X, Zhang L (2009) Parameter identifiability, constraint, and equifinality in data assimilation with ecosystem models. Ecol Appl 19:571–574
Luo Y, Ogle K, Tucker C, Fei S, Gao C, LaDeau S, Clark JS, Schimel DS (2011) Ecological forecasting and data assimilation in a data-rich era. Ecol Appl 21:1429–1442
Luo Y, Ahlström A, Allison SD, Batjes NH, Brovkin V, Carvalhais N, Chappell A, Ciais P, Davidson EA, Finzi A (2016) Toward more realistic projections of soil carbon dynamics by earth system models. Glob Biogeochem Cycles 30:40–56
Maag M, Vinther FP (1996) Nitrous oxide emission by nitrification and denitrification in different soil types and at different soil moisture contents and temperatures. Appl Soil Ecol 4:5–14
Menéndez S, Barrena I, Setien I, González-Murua C, Estavillo JM (2012) Efficiency of nitrification inhibitor DMPP to reduce nitrous oxide emissions under different temperature and moisture conditions. Soil Biol Biochem 53:82–89
Müller C, Stevens R, Laughlin R, Azam F, Ottow J (2002) The nitrification inhibitor DMPP had no effect on denitrifying enzyme activity. Soil Biol Biochem 34:1825–1827
Pan B, Lam SK, Wang E, Mosier A, Chen D (2021) New approach for predicting nitrification and its fraction of N_2O emissions in global terrestrial ecosystems. Environ Res Lett 16:034053
Pan B, Xia L, Lam SK, Wang E, Zhang Y, Mosier A, Chen D (2022) A global synthesis of soil denitrification: driving factors and mitigation strategies. Agric Ecosyst Environ 327:107850
Ruser R, Schulz R (2015) The effect of nitrification inhibitors on the nitrous oxide (N_2O) release from agricultural soils—a review. J Plant Nutr Soil Sci 178:171–188
Schädel C, Luo Y, David Evans R, Fei S, Schaeffer SM (2013) Separating soil CO_2 efflux into c-pool-specific decay rates via inverse analysis of soil incubation data. Oecologia 171:721–732
Senbayram M, Budai A, Bol R, Chadwick D, Marton L, Gündogan R, Wu D (2019) Soil NO_3^- level and O_2 availability are key factors in controlling N_2O reduction to N_2 following long-term liming of an acidic sandy soil. Soil Biol Biochem 132:165–173
Shi Z, Yang Y, Zhou X, Weng E, Finzi AC, Luo Y (2016) Inverse analysis of coupled carbon–nitrogen cycles against multiple datasets at ambient and elevated CO_2. J Plant Ecol 9(3):285–295
Stevens RJ, Laughlin RJ, Burns LC, Arah JRM, Hood RC (1997) Measuring the contributions of nitrification and denitrification to the flux of nitrous oxide from soil. Soil Biol Biochem 29(2):139–151
Tao F, Zhou Z, Huang Y, Li Q, Lu X, Ma S, Huang X, Liang Y, Hugelius G, Jiang L (2020) Deep learning optimizes data-driven representation of soil organic carbon in Earth system model over the conterminous United States. Front Big Data 3:17
Tao F, Huang Y, Hungate BA, Manzoni S, Frey SD, Schmidt MW, Reichstein M, Carvalhais N, Ciais P, Jiang L (2023) Microbial carbon use efficiency promotes global soil carbon storage. Nature 618:1–5
Trumbore SE (1997) Potential responses of soil organic carbon to global environmental change. Proc Natl Acad Sci USA 94:8284–8291
Weng E, Luo Y, Gao C, Oren R (2011) Uncertainty analysis of forest carbon sink forecast with varying measurement errors: a data assimilation approach. J Plant Ecol 4:178–191
Wolf U, Fuß R, Höppner F, Flessa H (2014) Contribution of N_2O and NH_3 to total greenhouse gas emission from fertilization: results from a sandy soil fertilized with nitrate and biogas digestate with and without nitrification inhibitor. Nutr Cycl Agroecosyst 100:121–134
Wrage N, Groenigen JV, Oenema O, Baggs E (2005) A novel dual-isotope labelling method for distinguishing between soil sources of N_2O. Rapid Commun Mass Spectrom Int J Rapid Dissem Res Mass Spectrom 19:3298–3306
Wu D, Senbayram M, Well R, Bruggemann N, Pfeiffer B, Loick N, Stempfhuber B, Dittert K, Bol R (2017) Nitrification inhibitors mitigate N_2O emissions more effectively under straw-induced conditions favoring denitrification. Soil Biol Biochem 104:197–207
Xia L, Lam SK, Chen D, Wang J, Tang Q, Yan X (2017) Can knowledge-based N management produce more staple grain with lower greenhouse gas emission and reactive nitrogen pollution? A meta-analysis. Glob Change Biol 23:1917–1925
Xia J, Wang J, Niu S (2020) Research challenges and opportunities for using big data in global change biology. Glob Change Biol 26:6040–6061
Xu T, White L, Hui D, Luo Y (2006) Probabilistic inversion of a terrestrial ecosystem model: analysis of uncertainty in parameter estimation and model prediction. Glob Biogeochem Cycles. https://doi.org/10.1029/2005GB002468
Xu X, Shi Z, Li D, Rey A, Ruan H, Craine JM, Liang J, Zhou J, Luo Y (2016) Soil properties control decomposition of

soil organic carbon: results from data-assimilation analysis. Geoderma 262:235–242

Yu L, Harris E, Lewicka-Szczebak D, Barthel M, Blomberg MR, Harris SJ, Johnson MS, Lehmann MF, Liisberg J, Müller C, Ostrom NE (2020) What can we learn from N_2O isotope data? Analytics, processes and modelling. Rapid Commun Mass Spectrom 34(20):e8858

Zebarth BJ, Forge TA, Goyer C, Brin LD (2015) Effect of soil acidification on nitrification in soil. Can J Soil Sci 95:359–363

Zerulla W, Barth T, Dressel J, Erhardt K, Horchler von Locquenghien K, Pasda G, Rädle M, Wissemeier A (2001) 3, 4-Dimethylpyrazole phosphate (DMPP)—a new nitrification inhibitor for agriculture and horticulture. Biol Fertil Soils 34:79–84

Zhou T, Luo Y (2008) Spatial patterns of ecosystem carbon residence time and NPP-driven carbon uptake in the conterminous United States. Glob Biogeochem Cycles. https://doi.org/10.1029/2007GB002939

Zhou ZY, Sun OJ, Luo ZK, Jin HM, Chen QS, Han XG (2008) Variation in small-scale spatial heterogeneity of soil properties and vegetation with different land use in semi-arid grassland ecosystem. Plant Soil 310:103–112

Zhou X, Luo Y, Gao C, Verburg PS, Arnone JA III, Darrouzet-Nardi A, Schimel DS (2010) Concurrent and lagged impacts of an anomalously warm year on autotrophic and heterotrophic components of soil respiration: a deconvolution analysis. N Phytol 187:184–198

Zhou X, Xu X, Zhou G, Luo Y (2018) Temperature sensitivity of soil organic carbon decomposition increased with mean carbon residence time: field incubation and data assimilation. Glob Change Biol 24:810–822